ISTITUTO NAZIONALE DI FISICA NUCLEARE
Laboratori Nazionali di Frascati

LNF-77/26(R)
30 Maggio 1977

M. Bassetti, A. Cattoni, A. Luccio, M. Preger and S. Tazzari:
A TRANSVERSE WIGGLER MAGNET FOR ADONE. -

Servizio Documentazione
dei Laboratori Nazionali di Frascati
Cas. Postale 13 - Frascati (Roma)

INFN - Laboratori Nazionali di Frascati
Servizio Documentazione

LNF-77/26(R)
30 Maggio 1977

M. Bassetti, A. Cattoni, A. Luccio(x), M. Preger and S. Tazzari:
A TRANSVERSE WIGGLER MAGNET FOR ADONE. -

INTRODUCTION. -

In the last few years, the installation of wiggler magnets on electron storage-rings has been proposed by several authors for two main purposes:

a) Beam size and polarization control, to improve the performance of colliding beam machines[5, 6].
b) Synchrotron light radiation enhancement and shift of its critical wavelength towards higher energies[9].

Wigglers required for the two above applications are in principle of quite different types. For beam size control applications conventional magnets with a few poles (2 full poles) are usually sufficient, while to fully exploit the capabilities of a wiggler for synchrotron radiation, high-field superconducting magnets with a large number of poles are required.

It is a fact however that not enough experimental information is available on either type. In the very few cases where wiggler-like devices have been operated in connection with storage rings (damper magnet at CEA[1], experimental wigglers at Wisconsin[2], MEA magnet at Adone[3]) they were too special to really provide all the relevant information.

Therefore, quite apart from the results to be obtained in terms of applications a) and b) above, we think it would be of general interest to have a wiggler magnet installed soon on a storage ring in operation.

In this general frame the present proposal, a conventional wiggler magnet to be installed on Adone, has the following advantages:

a) Limited cost and possibility of fast commissioning since a free straight section is available and it is planned to power the magnet from existing power supplies.
b) Lowering of the synchrotron radiation critical wavelength from 8.3 A to 4.6 A, i.e. to the value that would be obtained if the ring could be operated at $\sim$2 GeV. (Source intensity could also be increased by a factor of up to 5).
c) Detailed study of the effects on beam dimensions and damping rates (possibility of increasing the injection rate into the ring).
d) Possibility, by later addition of a second wiggler, of a considerable increase in luminosity at low energy, in two of the present four interaction regions.

(x) - Università degli Studi, Pisa.

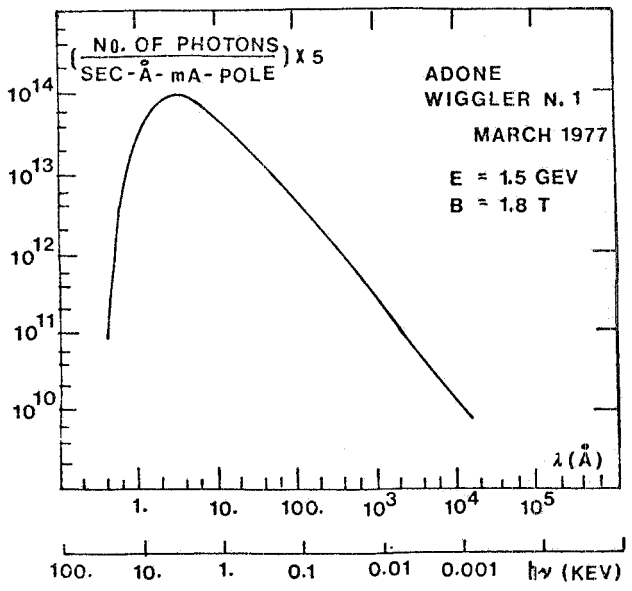

FIG. 1

We do not intend here to go into the details of synchrotron radiation physics applications that have been extensively covered elsewhere[4]. The expected synchrotron light spectrum at 1.5 GeV is given in Fig. 1.

A somewhat detailed treatment of the linear effects of the wiggler on the machine is instead given in the first part of this paper, so that the discussion of the proposal may be more easily understandable.

PART I - LINEAR OPTICS OF WIGGLER MAGNETS. -

I. 1. - Transport matrix in the plane normal to the field. -

Let the field in the wiggler be schematized as shown in Fig. 2, assuming there are n full poles.

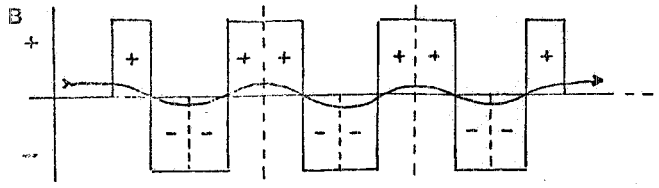

FIG. 2

The overall wiggler matrix can be obtained from that, B, of the first half-pole as follows:

Define matrices

$$R = \begin{vmatrix} 1 & 0 & 0 \\ 0 & -1 & 0 \\ 0 & 0 & 1 \end{vmatrix}, \quad S = \begin{vmatrix} -1 & 0 & 0 \\ 0 & -1 & 0 \\ 0 & 0 & 1 \end{vmatrix}, \quad B = \begin{vmatrix} b_{ij} \end{vmatrix} \qquad i,j = 1\text{-}3 \qquad (1)$$

and

$$B_R = RB^{-1}R \, .$$

Matrix S is introduced to describe the inverse polarity half-poles.

The second half-pole matrix is then SB_RS, the third half-pole matrix is SBS and the fourth half-pole one is B_R. Since the first four half-poles are obviously a subperiod of the whole wiggler, the overall wiggler matrix is

$$W = (B_R SBB_R SB)^{n/2} \, . \qquad (2)$$

It can be furthermore seen from (2) that the periodicity is actually n, and one can write

$$W = (B_R S B)^n \quad . \tag{3}$$

All the relevant information is thus contained in the matrix

$$P = B_R S B \, . \tag{4}$$

b_{ij} being the elements of B ($b_{31} = b_{32} = 0$, $b_{33} = 1$) and calling P_{ij} those of P, it follows from (1) and (4) that

$$\begin{aligned} P_{11} &= -(b_{11}b_{22} + b_{12}b_{21}) = P_{22} \, , & P_{13} &= -2B_{22}b_{13} \, , & P_{33} &= 1 \, . \\ P_{12} &= -2b_{12}b_{22} \, , & P_{23} &= -2B_{21}b_{13} \, , & & \\ P_{21} &= -2b_{21}b_{11} \, , & P_{31} &= P_{32} = 0 \, , & & \end{aligned} \tag{5}$$

The negative sign of the first six elements is due to the fact that, at the exit of the second half--pole, coordinates are referred to the (negative) pole inverted reference.

Assuming the wiggler field in each pole section to be constant along the normal to the field (coordinate x), whereby the matrix must be invariant against shifts along the x axis, it is found that

$$b_{21} = 0 \tag{6}$$

giving :

$$P_{21} = P_{23} = 0 \, , \qquad P_{11} = P_{22} = -1 \, , \tag{6'}$$

and that (see Fig. 3) :

$$b_{11} = \cos\varphi \, , \tag{6"}$$

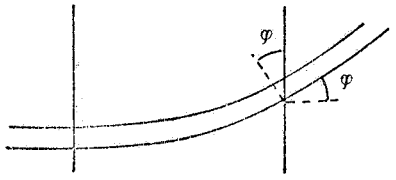

FIG. 3

where φ is the trajectory bending angle produced by a half--pole.

From (6") and (6) it follows that

$$b_{22} = 1/\cos\varphi \, , \tag{7}$$

so that the only relevant element left undetermined is b_{12} (elements P_{13} and P_{23} cancel out when matrix P is squared).

From (2) and (3) it follows that :

$$W = (P^2)^{n/2}$$

with

$$P^2 = \begin{vmatrix} 1 & 4b_{12}b_{22} & 0 \\ 0 & 1 & 0 \\ 0 & 0 & 1 \end{vmatrix} \, , \tag{8}$$

so that, under the assumption made, the wiggler matrix is simply that of a straight section.

To compute its effect on the machine it is useful to transform it so that it is equivalent to a perturbation localized at the wiggler center point, which is simply done by multiplying W, to the right and to the left, by the inverse of a straight section matrix having a (negative) length equal to one half the wiggler magnet overall length.

The result is

$$W = \begin{vmatrix} 1 & 2n(b_{12}b_{22} - 1 & 0 \\ 0 & 1 & 0 \\ 0 & 0 & 1 \end{vmatrix} , \tag{9}$$

1 being the length of one half-pole.

One then has, to a good approximation

$$b_{12} = \varrho_w \sin \varphi \ , \tag{10}$$

ϱ_w being the trajectory radius of curvature in the wiggler. Furthermore, since

$$1 = \varrho_w \sin \varphi \ , \qquad \text{and} \qquad b_{22} = 1/\cos \varphi \ , \tag{11}$$

it is found that

$$W_{12} = \Delta 1 = 2n\,(b_{12}b_{22} - 1) = 2n\,\varrho_w (\mathrm{tg}\,\varphi - \sin \varphi) \simeq \frac{n 1^3}{\varrho_w^2} \ . \tag{12}$$

The $\Delta 1$ given by (12) is that appearing in W and determining the effect of the wiggler on betatron oscillations.

The actual lengthening of the reference trajectory, ΔC, is given by

$$\Delta C = 2n\,(\varrho_w \varphi - \varrho_w \sin \varphi) \simeq n \frac{\varrho_w}{3} \left(\frac{1}{\varrho_w} \right)^3 \ , \tag{13}$$

and is three times smaller than $\Delta 1$.

I. 1. 1. - Effects of the dependence of B on the x coordinate.

The assumption has been made that the wiggler field in each pole section is constant along x (coordinate normal to the field), i. e.

$$\frac{\partial B}{\partial x} = 0 \ .$$

Actually, due to the finite aperture, this is not exactly true. The effect has to be taken into account. Let us call z the coordinate parallel to the field direction, and let us assume that

$$I = \int_0^L B_z(x, s)\, ds \Big|_{x=\mathrm{const}} = 0 \tag{14}$$

independent of x. However, in order to calculate the effect of the wiggler on the particle motion, the relevant integral is not I but the integral taken along the actual particle trajectory, for which x is not constant. With the additional reasonable assumption that the particle trajectory slope at the wiggler entry point, x'_{in}, is much smaller than angle φ (see Fig. 3)

$$x'_{in} \ll \varphi = \frac{1}{\varrho_w} \tag{15}$$

let's assume that the dependence of B_z on s and x can be factorized as follows:

$$B(s, x) = B(s)\left[1 + g(x)\right] \quad , \tag{16}$$

with $g(x) \ll 1$.

One has to consider that the non zero part of the integral along the actual particle trajectory δI, comes from two effects: the change in B and the change in path length. Both effects cause the bending angle at the exit of a pair of half poles to change by some $\delta\varphi$, and we want to calculate the overall $\Delta\varphi$. Assuming the particle trajectory to consist of circumference arcs plus straights, the situation is shown in Fig. 4.

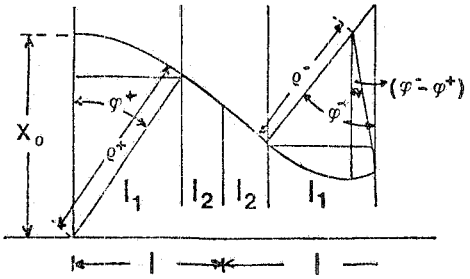

FIG. 4

Since

$$\varrho_w^+ \sin\varphi^+ = \varrho_w^- \sin\varphi^+ + \varrho_w^- \sin(\varphi^- - \varphi^+) \tag{17}$$

apart from higher order terms one has

$$\Delta\varphi = (\varphi^- - \varphi^+) = \frac{\varrho_w^+ - \varrho_w^-}{\varrho_w^-}\,\varphi^+ = \frac{B^- - B^+}{B^+}\,\varphi^+ \quad . \tag{18}$$

Using (16), one may write

$$\Delta\varphi \cong \varphi^+\left[g(x^-) - g(x^+)\right] \simeq \varphi\left[g(x^-) - g(x^+)\right] \quad , \tag{19}$$

where x^+ and x^- are two particular values of x whose difference is less than the peak-to-peak amplitude of the wiggle. Let us write

$$x^+ = x_o + qA \quad , \qquad x^- = x_o - qA \quad , \tag{20}$$

q being the proper factor to be applied to A, wiggle peak amplitude.

Assuming g(x) is an even function of x

$$g(x) = ax^2 + bx^4 + cx^6 + \cdots \tag{21}$$

and substituting into (19) one obtains

$$\Delta\varphi = -\varphi\left[(4qAa + 8q^3A^3b)\,x_o + 8qAb\,x_o^3 + \cdots\right] \quad . \tag{22}$$

To first order in x_o the perturbation is equivalent to a distributed quadrupole, giving rise to an element W_{21} in (9). One has

$$W_{21} \simeq -n\frac{\partial\Delta\varphi}{\partial x_o} = -(4aqA + 8bq^3A^3)\,n\varphi + \cdots \tag{23}$$

and the corresponding tune shift will be

$$\Delta Q_x \simeq -\frac{\beta_x W_{21}}{4\pi} \quad . \tag{24}$$

Needless to say, if A vanishes, so does W_{21}.

In order to obtain an estimate of the effect, let us write, in smooth approximation

$$\left| x''(s) \right| = \left| \frac{1}{\varrho_w} \right| = \left(\frac{2\pi}{\lambda_w}\right)^2 A \quad , \qquad \lambda_w = 4l \quad , \tag{25}$$

so that, in terms of ϱ_w and l, one may write

$$A \approx \left(\frac{\lambda_w}{2\pi}\right)^2 \frac{1}{\varrho_w} = 4 \frac{l^2}{\pi^2 \varrho_w} \quad , \qquad \varphi \simeq \frac{l_1}{\varrho_w} \tag{26}$$

(l_1 is the half pole magnetic length in a rectangular model; see Fig. 5).

Substituting (26) into (24) one finally obtains:

$$\Delta Q_x \cong n \frac{4l^2 l_1 \beta_x}{-\pi^3 \varrho_w^2} q \left(a + \frac{32}{\pi^4} q^2 \frac{l^4}{\varrho_w^2} b\right) . \tag{27}$$

Since usually $b \lesssim a$, the second term is much smaller than the first and may be neglected.

On the other hand, at large amplitudes of oscillation such as those one would have if one tried to inject with the wiggler on, the next term in (23), giving rise to a

$$\Delta Q_x^{(2)} \cong n \frac{24 l^2 l_1}{\pi^3 \varrho_w^2} q \left(b x_o^2\right) \beta_x \tag{28}$$

may become important.

I. 2. - Transport matrix in the field plane.

In the plane of the magnetic field, matrix dimensions reduce to 2 x 2 so that matrix S (see I. 1) is no longer necessary.

However, although the periodicity considerations made earlier remain true, the half pole matrix is now more dependent on the details of the magnetic field.

Let us describe the half pole matrix, in a very general way, as follows

$$B_2 = \begin{vmatrix} b_{44} & b_{45} \\ b_{54} & b_{55} \end{vmatrix} . \tag{29}$$

From (5) we obtain, eliminating the "-" sign that was due to transformation S

$$P_{44} = P_{55} = b_{44}b_{55} + b_{45}b_{54} , \quad P_{12} = 2 b_{45} b_{55} , \quad P_{21} = 2 b_{54} b_{44} . \tag{30}$$

Matrix P_2 can obviously be written in the following form

$$P_2 = \begin{vmatrix} P_{44} & P_{45} \\ P_{54} & P_{55} \end{vmatrix} = \begin{vmatrix} \cos\theta & \beta \sin\theta \\ -\frac{\sin\theta}{\beta} & \cos\theta \end{vmatrix} .$$

By taking the n^{th} power of P_2 one obtains

$$W_2 = \begin{vmatrix} \cos n\theta & \beta \sin n\theta \\ -\dfrac{\sin n\theta}{\beta} & \cos n\theta \end{vmatrix} \tag{31}$$

and multiplying to the right and to the left by the matrix of a $(-nl)$ long straight section one eventually has

$$W_2^* = \begin{vmatrix} \cos n\theta + \dfrac{nl}{\beta} \sin n\theta & \sin n\theta \left[\beta - \left(\dfrac{nl}{\beta}\right)^2\right] - 2nl \cos n\theta \\ -\dfrac{\sin n\theta}{\beta} & \cos n\theta + \dfrac{nl}{\beta} \sin n\theta \end{vmatrix} \tag{32}$$

which, at least for not too high field values, can again be put into the form

$$W_2^* = \begin{vmatrix} \cos \theta^* & \beta^* \sin \theta^* \\ -\dfrac{\sin \theta^*}{\beta^*} & \cos \theta^* \end{vmatrix} . \tag{33}$$

I. 2. 1. - The matrix for a rectangular field model.

Lets calculate matrix W_2^* with the following rectangular field model (Fig. 5) .

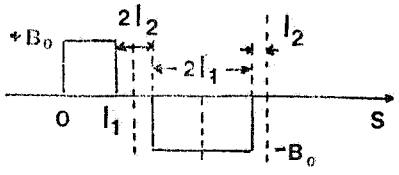

FIG. 5

The value l_1 is chosen so that

$$B_o l_1 = \int_0^{l_1} B(s)\, ds$$

B_o being the nominal field in the wiggler. l_2 is chosen so that $l_1 + l_2 = 1$.

It can be found with some algebra that

$$B_2 = \begin{vmatrix} 1 - tl_2 & l_1 + l_2 - tl_1 l_2 \\ -t & 1 - tl_1 \end{vmatrix} \tag{34}$$

and

$$P_2 = \begin{vmatrix} 1 - 2t(l_1+l_2) + 2t^2 l_1 l_2 & 2\left[l_1+l_2 - t(l_1^2 + 2l_1 l_2) + t^2 l_1^2 l_2\right] \\ -(t - t^2 l_2) & 1 - 2t(l_1+l_2) + 2t^2 l_1 l_2 \end{vmatrix} \tag{35}$$

where

$$t = tg\varphi / \varrho_w .$$

It is not worthwhile to try further expliciting P_2 because the physical picture does not become any simpler. On the other hand, starting from the above formulae it is easy to obtain β^* and θ^* by means of a computer program. As an example, the behaviour of these two functions versus

ϱ_w for the magnet design described in Part II, is shown in Fig. 6.

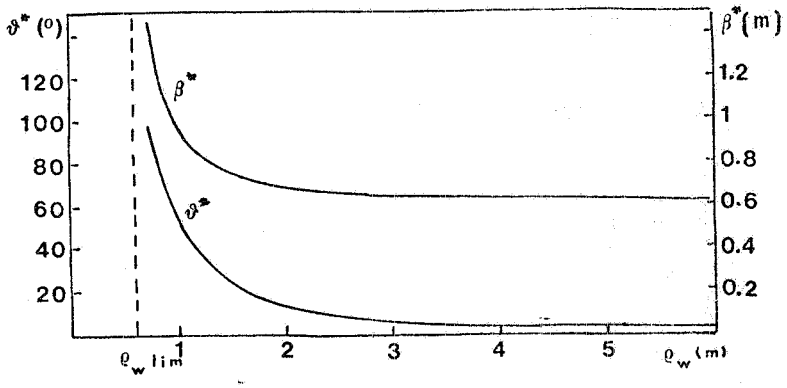

FIG. 6

It can be seen from the figure and from (33) that when ϱ_w tends to infinity, matrix W_2^* tends to the identity matrix I, while the value of β^* tends to (see Appendix I)

$$\lim_{\varrho_w \to \infty} \beta^* = \left[\frac{(n^2 - 1) l^2}{3} + l_2^2 \right]^{1/2} \tag{36}$$

with the usual meaning of the symbols.

Also, when ϱ_w is decreased towards zero, at some point each pair of half poles produces a π/n rotation in betatron phase space so that the overall matrix becomes (-I). For the rest of the ring this is equivalent to removing a straight section length $2 \cdot n \cdot l$.

The value of ϱ_w for which this occurs is somehow a limit value and is given by (as can be deduced from P_{44} of (35)):

$$\varrho_{w_{lim}} \simeq \frac{\sqrt{l l_1}}{\sin \frac{\pi}{2n}} \quad . \tag{37}$$

I. 2. 2. - Matching.

Assume the unperturbed ($\varrho\omega = \infty$) one-turn matrix, starting from the symmetry point opposite to the wiggler (or in between two wigglers), is given by

$$M_o \, e^{J \mu} \quad . \tag{38}$$

When the wiggler is turned on, this becomes

$$M_w = e^{J\mu/2} \, e^{J^* \varrho^*} \, e^{J\mu/2} \quad . \tag{39}$$

By setting

$$M_w = \begin{vmatrix} \cos \mu_w & \beta_w \sin \mu_w \\ -\frac{\sin \mu_w}{\beta_w} & \cos \mu_w \end{vmatrix} \tag{40}$$

one finds, with some algebra

$$\cos \mu_w = \cos(\mu + \theta^*) - \sin \mu \sin \theta^* \frac{(\beta^* - \beta_o)^2}{2 \beta_o \beta^*}$$

$$\beta_w = \frac{\beta_o}{\sin \mu_w} \left\{ \sin \mu_w + (\beta^* - \beta_o) \sin \theta^* \left[\frac{\cos^2 \mu/2}{\beta_o} + \frac{\sin^2 \mu/2}{\beta^*} \right] \right\} \tag{41}$$

where β^*, θ^* are those defined by (33), and β_o, μ are those of the unperturbed machine.

From (41) it can be seen that if

$$\beta^* = \beta_o ,$$

then

$$\mu_w = \mu + \theta^* , \qquad \beta_w = \beta_o = \beta^* , \tag{42}$$

so that a perfect match is obtained.

Furthermore, when $\theta^* \to 0$, no matter what the value of β^*, one has as expected

$$\mu_w = \mu , \qquad \beta_w = \beta_o .$$

In the general case where $\theta^* \neq 0$, $\beta^* \neq \beta$ a stopband is produced. The stopband is defined as the interval of μ in which $|\cos \mu_w| > 1$.

By setting

$$h = 1 + \frac{(\beta^* - \beta_o)^2}{2 \beta_o \beta^*} \tag{43}$$

it is found that the two boundary points of the stopband are given by

$$\text{tg}\, \mu/2 = - \text{tg} \frac{\theta^*}{2} \left[h \pm \sqrt{h^2 - 1} \right] \qquad \text{for} \quad \mu = 2k$$

or

$$\text{tg}\, \mu/2 = \text{cotg} \frac{\theta^*}{2} \left[h \pm \sqrt{h^2 - 1} \right] \qquad \text{for} \quad \mu = (2k+1) . \tag{44}$$

From (43), (44) it can be deduced that the stopband width

$$\Delta \mu \simeq 2 \, \text{tg} \frac{\theta^*}{2} \sqrt{h^2 - 1} \tag{45}$$

tends to zero when $\beta^* \to \beta$, giving a perfect match as already shown above.

Whenever a mismatch exists, the unperturbed β function is distorted. It can be shown (see Appendix II) that the resulting ripple in the β function can be evaluated as follows

$$\Delta \beta(s) = \frac{\beta(s)}{\beta_o} (\beta_w - \beta_o) \left[1 - \sin^2 \mu(s) \left(1 + \frac{\beta_o}{\beta_w} \right) \right] \tag{46}$$

where β_o, $\beta(s)$, $\mu(s)$ are unperturbed machine values. $\mu(s)$ is measured, according to the position made at the beginning of the paragraph, starting from a symmetry point (e. g. the point opposite to the wiggler) and β_o is the unperturbed β function value at that point.

From (46) we obtain the following inequalities

$$\frac{\beta(s)}{\beta_w}(\beta_o - \beta_w) < \Delta\beta(s) \leq (\beta_w - \beta_o)\frac{\beta(s)}{\beta_o} \qquad \text{if } \beta_w > \beta_o$$

$$\frac{\beta(s)}{\beta_o}(\beta_w - \beta_o) \leq \Delta\beta(s) \leq (\beta_o - \beta_w)\frac{\beta(s)}{\beta_w} \qquad \text{if } \beta_w < \beta_o . \tag{47}$$

PART II - PROPOSED WIGGLER(S) FOR ADONE.

II. 1. - Magnet design. -

II. 1. 1. - Gap height.

The wiggler magnet will be installed in one of the four 2.5 m long interaction straights of Adone.

It is of course crucial to determine the minimum gap height compatible with the present way of operation of the machine, both at injection and in the colliding beam mode. One way of doing this is the following: the present vertical aperture limit in the machine is at an F quadrupole next to a non-interaction straight (in which the vertical fast feedback electrodes are mounted), at a point where $\beta_z = 8.8$ m. The limit aperture is ~ 50 mm.

If one traces this value back to the edge of the interaction straight where the wiggler will sit, taking into account the requirement that in the present mode of operation the beams be separated by ~ 14 mm in all straights at injection (300 MeV); one finds that the equivalent aperture required at the wiggler ($\beta_z = 3.8$ m) is

$$a_{ss} \simeq 37 \text{ mm}.$$

With this aperture normal machine operation should remain unchanged.

Given this requirement, a round figure of 40 mm has been specified for a magnet gap, leaving an available aperture of ~ 35 mm instead of the computed 37 mm. With careful alignement of the magnet and possibly a better vertical closed orbit correction, we believe that normal machine operation will still remain practically unaffected.

Anyway the magnet is so designed that, if necessary, the aperture can easily be increased by $\sim 10\%$ at the expense of a slight decrease in the maximum field. It will be shown in the following that the proposed aperture is also compatible with operation in the colliding beam mode with two wigglers.

II. 1. 2. - Specifications.

The design aims are:

- 6 full poles ,
- Max field 18 kG ,
- Useful horizontal aperture 200 mm + space required for trajectory inside wiggler,

The useful aperture is defined as the region where $\Delta B/B_o \leq 10^{-3}$.

The constraints are:

- Existing power supply output: 400 V d. c., 5000 A,
- Existing cooling system pressure: 6 atm at the magnet manifolds,
- Gap height $h \geq 40$ mm (due to the vertical aperture needed by the machine),
- Overall length ≤ 2300 mm.

The design meets the following specifications:

- Iron saturation at the yoke By $\leq$ 15 KGauss,
- Iron saturation at the pole base (minimized by tapering) Bp $\simeq$ 16 KGauss,
- Conductor current density J ≤ 20 A/mm^2 max,
- Coil filling factor: $\sim 50\%$,
- Pole width at the gap given by

$$W = Wu + 1.5\,h + 2\,f\,,$$

where Wu = horizontal useful aperture (200 mm) and f = trajectory sagitta (≤ 1 cm).

The mechanical and main dimensional specifications of the magnet are summarized in Table I.

TABLE I - Magnet specifications

Number of poles	5 full poles, 2 half poles
Gap height	40 mm
Field at pole center	18 KGauss
Total flux per pole	0.181 Wb
Flux dispersion	$\sim 33\%$ of total flux
Ampereturns per pole	31500
Current	4500 A
Voltage accross all coils in series	42 V
Overall power	189 KW
Water flow	190 l/min
Temperature rise	$\sim 15^{\circ}$C
Iron weight	$\sim$5100 Kg
Copper weight	$\sim$270 Kg
Overall magnet length	2100 mm

Fig. 7 shows a horizontal section through the pole. The side plates on which the top pole piece sits are aluminum.

Fig. 8 shows a side view of the magnet.

The performance of the magnet has been simulated by means of the CERN "Poisson" program and found to be quite satisfactory. Further work is in progress to optimize details of the transverse useful aperture and longitudinal field integral.

The two end half-poles are equipped with an extra turn, providing a fine adjustement of the field integral via a separate small power supply. The existing MEA compensator power supply allows the field integral to be corrected by as much as $\pm$ 35 Gauss - m.

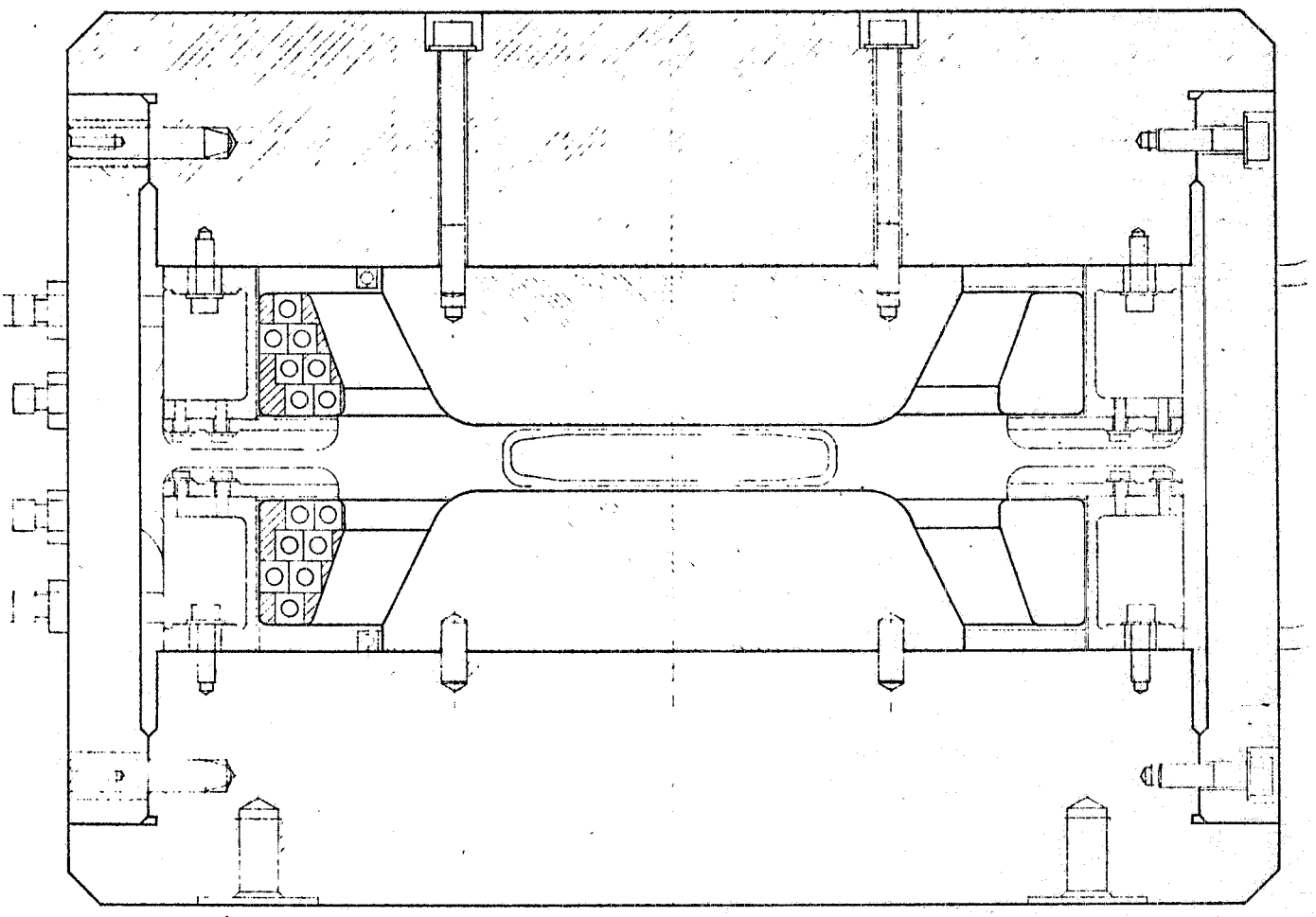

FIG. 7

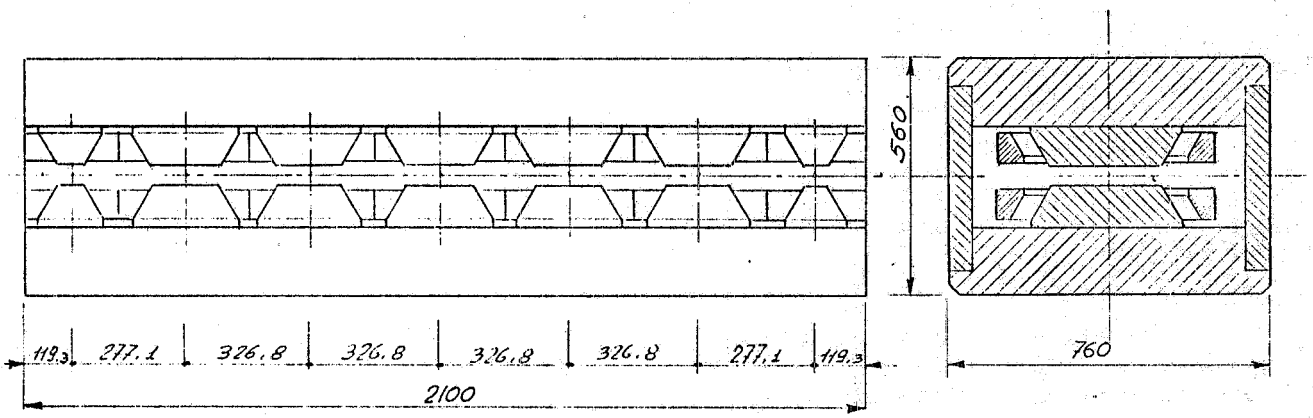

FIG. 8

II. 1. 3. - Reference trajectory.

A sketch of the reference trajectory inside the wiggler is shown in Fig. 9. The maximum deviation from the unperturbed reference orbit, in a rectangular model like the one shown above, is given by

$$2A = \frac{\lambda_w^2}{16} \left(1 - \frac{l_2^2}{(l_1 + l_2)^2}\right) \tag{48}$$

l_1 being the half-pole magnetic length and l_2 the half distance between neighbouring poles.

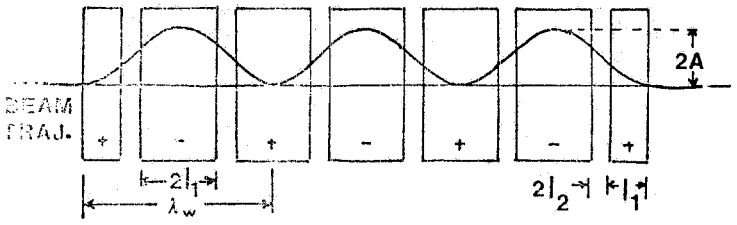

Wiggler straight section FIG. 9

With our parameters:

$$l_1 \simeq 13.4 \text{ cm}, \qquad l_2 \simeq 4.6 \text{ cm}, \qquad \lambda_w = 4(l_1 + l_2) = 41 \simeq 72 \text{ cm},$$

one has

$$2A_{(cm)} = 3 \frac{1}{\varrho_{w(m)}} \ . \tag{49}$$

Assuming the field is kept constant at 18 KG, ϱ_w is given in terms of machine energy, by

$$\varrho_{w(m)} = 1.85 \, E_{(GeV)} \ . \tag{50}$$

II. 2. - Matching.

As shown in Part I of this paper, an ideal wiggler magnet leaves the horizontal plane of the machine practically unaffected but has considerable effect on the vertical plane.

In particular θ^* and β^* of formula (37) have been computed for the proposed magnet and found to be (see Fig. 6):

$$\theta^*(\varrho_w = 1 \text{ m}) = 52.8^\circ, \qquad \beta_z^*(\varrho_w = 1 \text{ m}) = 0.956 \text{ m}. \tag{51}$$

Since the β_z value of the unperturbed machine at its normal operating point ($Q_x \simeq Q_z = 3.1$) is 3.1 m, it is clear from (41) (42) that there is a large mismatch. The resulting stopband width is (see (45))

$$\Delta\mu \simeq 99^\circ \ .$$

On the other hand, given our lattice, the best way of changing the unperturbed β_z is that of changing Q_z.

We find that by running the Q_z value up to $\simeq 5.2$, β_z at the interaction point becomes

$$\beta_z = 0.922 \qquad (Q_z = 5.2) \ .$$

The resulting mismatch is very small, the stopband width being:

$$\Delta\mu \simeq 2.1^{o} \ . \tag{52}$$

The limit value of ϱ_w as defined by (37), is for our case

$$\varrho_{w(cm)} \cong 0.6 \text{ m} \ .$$

Fig. 10 shows the behaviour of the β_z function within the wiggler straight section, as a function of ϱ_w, at the new operating point ($Q_x \simeq 3.2$, $Q_z \simeq 5.2$), as obtained using formula (A7)). Tests on the injection of an electron beam on the new operating point have already been successfully carried out.

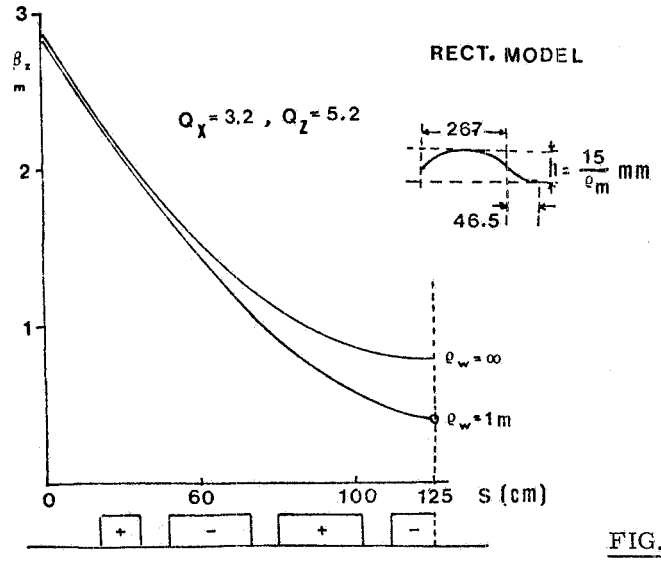

FIG. 10

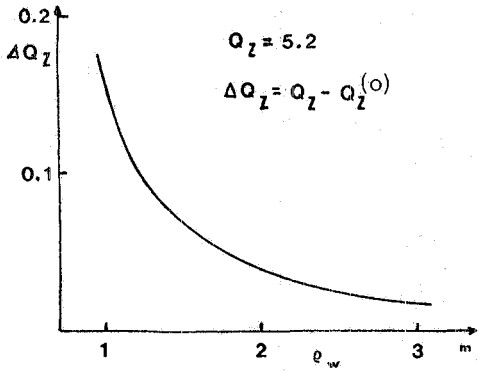

FIG. 11

Of course θ^* also produces a shift in θ_z (see (42)) than can be compensated for by means of the ring quadrupoles. The value of

$$\Delta Q_z = Q_z - Q_z^{(o)}$$

is plotted versus ϱ_w in Fig. 11.

It is worthwhile to add that the path lengthening due to the wiggler is (see (13)) for our case:

$$\Delta C \simeq n \frac{\varrho_w}{3} \left(\frac{1}{\varrho_w}\right)^3 = 9.5 \times 10^{-3} \ \frac{1}{\varrho_w^2(m)} \ \text{m} \tag{53}$$

i.e. 9.5 mm in the worst case ($\varrho_w = 1$ m), which is negligible from the point of view of the required RF frequency adjustment ($\Delta f/f \simeq 10^{-4}$).

The change in momentum compaction is

$$\frac{\Delta\alpha_c}{\alpha_c} = -\frac{1}{\alpha_c} \ \frac{2n}{3} \frac{1}{L} \left(\frac{1}{\varrho_w}\right)^2 \simeq 3 \times 10^{-3} \ , \tag{54}$$

where L is the overall length of the orbit, and is therefore also negligible.

II. 3. - Tolerances

II. 3. 1. - Field integral.

By means of the correction windings the field integral can be reduced to zero provided the fabrication tolerance does not exceed $\pm$ 35 G-m.

However a residual plane-parallel lens effect remains, even after the field integral has been corrected, if individual magnet poles do not exibit the ideal simmetry characteristics. The effect can be estimated as follows.

A field integral error ΔI, can be assumed to be equivalent to an angular perturbation

$$\delta = \frac{e}{p} \Delta I \, . \tag{55}$$

The following model can then be used (see Fig. 12). The residual fabrication error on the field integral is assumed to be equivalent to an angular discontinuity δ_2 located at some point χ along the wiggler. L is the overall wiggler length. At both ends of the wiggler there is a correction angular discontinuity, δ_1, produced by the correction windings on the end half-poles.

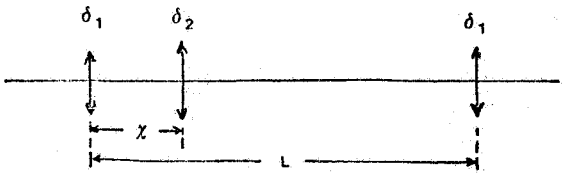

FIG. 12

If the vector at the wiggler input is

$$\begin{vmatrix} x_o \\ x'_o \end{vmatrix}$$

the output vector will be

$$\begin{vmatrix} x \\ x' \end{vmatrix} = \begin{vmatrix} x_o + x'_o L + L\delta_1 + (L - \chi)\delta_2 \\ x'_o + 2\delta_1 + \delta_2 \end{vmatrix} \tag{56}$$

After correction, one will have :

$$2\delta_1 = -\delta_2 \, , \tag{57}$$

so that substituting into (56) the output vector becomes

$$\begin{vmatrix} x \\ x' \end{vmatrix} = \begin{vmatrix} x_o + x'_o L \\ x'_o \end{vmatrix} + \begin{vmatrix} (\frac{L}{2} - \chi)\delta_2 \\ 0 \end{vmatrix} \tag{58}$$

evidentiating the equivalence of the model to a plane-parallel lens. As expected, if a symmetry point exists ($\chi = L/2$) the effect vanishes.

For a worst-case estimate one can set $\chi = 0$ and obtain:

$$\Delta x = x - (x_o + x'_o L) = \frac{L}{2} \delta_2 \, . \tag{59}$$

As it is well known the Δx will produce a closed orbit whose apmlitude A is given by

$$A = \frac{\Delta x}{2 \sin \pi \Delta Q_x} \qquad \text{with} \qquad \Delta Q_x = Q_x - \text{INT}(Q_x) \tag{60}$$

Using (55) and (59), (60) can be solved for ΔI, yielding

$$\Delta I = \frac{e}{p} \frac{4 A \sin \pi \Delta Q_x}{L} \quad . \tag{61}$$

Assuming $\Delta Q_x = 0.05$, $L = 2$ m and $A \leq 2$ mm one obtains a tolerance on fabrication errors

$$\Delta I \lesssim 20 \text{ Gauss} - \text{m} \quad . \tag{62}$$

II. 3. 2. - Field uniformity in the radial plane.

Assume the field at a distance x from the unperturbed machine reference orbit is given by (see (21)) :

$$B(x) = B_o (1 + ax^2 + bx^4 + \cdots) \quad . \tag{63}$$

The effects described in section I. 1. 1 set a limit on the maximum allowed values of a and b.

With a rectangular model where $l \cong 18$ cm, $l_1 \cong 13.4$ cm one obtains from (27) (by neglecting the second term, imposing $\Delta Q_{x\,max} \approx 2 \times 10^{-3}$ and setting $q \simeq 1$) :

$$2 \times 10^{-3} \approx n \frac{4 l^2 l_1^2}{\pi^3 \varrho_w^2} \beta_x a \cong 7 \times 10^2 a \quad (\text{cm}^{-2})$$

in the worst case ($\varrho_w = 1$ m, $\beta_x = 10.8$ m). Therefore a must satisfy the equation

$$a \lesssim 3 \times 10^{-6} \text{ cm}^{-2} \quad . \tag{64}$$

At large oscillation amplitudes, evaluating formula (28) at $x_o = 10$ cm, and assuming that a ΔQ_{max} of $\sim 2 \times 10^{-2}$ can be tolerated, one has

$$b_{max} \lesssim 3 \times 10^{-8} \text{ cm}^{-4} \quad . \tag{65}$$

With these values, at the edge of the useful aperture ($x_o \simeq 10$ cm) one should have

$$\left. \frac{B - B_o}{B_o} \right|_{max} \simeq a_{max} x_o^2 + b_{max} x_o^4 \lesssim 10^{-3} \quad . \tag{66}$$

II. 4. - Effects on damping, momentum spread and emittance.

For our machine and the proposed wiggler a smooth-approximation calculation shows that the damping partition coefficients are unchanged (to an accuracy of better than 10^{-3}). Therefore, given the unperturbed machine damping time τ_o, the damping time with wiggler is reduced by the factor[1, 2]

$$\frac{\tau_w}{\tau_o} = \left(1 + \frac{\varrho_M^2}{\varrho_w^2} \frac{l_w}{l_M}\right)^{-1} \quad , \tag{67}$$

where l_w, l_M are the magnetic lengths of the wiggler and the lattice magnets respectively, and ϱ_w, ϱ_M are the magnetic radii of curvature in the wiggler and the lattice magnets respectively.

The perturbed to unperturbed momentum spread ratio $(\sigma p/\sigma p_o)$ is given by formula[5, 6]

$$\left(\frac{\sigma_p}{\sigma_{p_o}}\right)^2 = \frac{1 + \frac{l_w}{l_M}\left(\frac{\varrho_M}{\varrho_w}\right)^3}{1 + \frac{l_w}{l_M}\left(\frac{\varrho_M}{\varrho_w}\right)^2} \tag{68}$$

where the symbols have been defined above.

In order to calculate the effect of the wiggler on the emittance it is necessary to know how the invariant $\mathscr{H}$[7] transforms. The invariant with wiggler $(\mathscr{H})$ is related to that of the unperturbed machine $(\mathscr{H}_o)$ by the formula

$$\frac{\mathscr{H}}{\mathscr{H}_o} = \frac{1 + \frac{l_w}{l_M}\left(\frac{\varrho_M}{\varrho_w}\right)^3 \frac{\mathscr{H}_w}{\mathscr{H}_o}}{1 + \frac{l_w}{l_M}\left(\frac{\varrho_M}{\varrho_w}\right)^3} \tag{69}$$

where $\mathscr{H}_w$ is the invariant calculated over the wiggler magnetic field region[6].

Finally the ratio of perturbed to unperturbed emittances is given by

$$\frac{\varepsilon_{x\beta}}{\varepsilon_{x\beta_o}} = \frac{\varepsilon_z}{\varepsilon_{z_o}} = \frac{\sigma_p^2}{\sigma_{p_o}^2}\frac{\mathscr{H}}{\mathscr{H}_o} = \frac{1 + \frac{l_w}{l_M}\left(\frac{\varrho_M}{\varrho_w}\right)^3 \frac{\mathscr{H}_w}{\mathscr{H}_o}}{1 + \frac{l_w}{l_M}\left(\frac{\varrho_M}{\varrho_w}\right)^2} \quad . \tag{70}$$

The vertical emittance is directly given by (70) while, in order to obtain the actual radial emittance, ε_x, one must add the synchrotron contribution, namely

$$\varepsilon_x = \varepsilon_{x\beta} + \sigma_p^2 \frac{\eta^2}{\beta_x} \quad .$$

Ratios τ_w/τ_o, $(\sigma_p/\sigma_{p_o})^2$, $\mathscr{H}/\mathscr{H}_o$ and $\varepsilon_z/\varepsilon_{z_o}$ are plotted versus ϱ_w, for our case, in Fig. 13a.

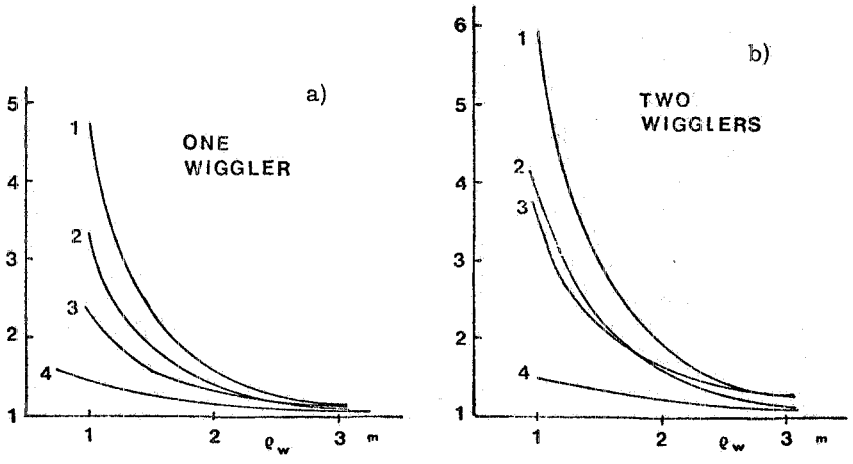

Curve 1 - $\varepsilon_z/\varepsilon_{z_o}$

Curve 2 - $\sigma_p^2/\sigma_{p_o}^2$

Curve 3 - τ_{D_o}/τ_D

Curve 4 - $\mathscr{H}/\mathscr{H}_o$

FIG. 13

It can be seen from (70) that in principle, $\varepsilon_z / \varepsilon_{z_o}$ can be made less than 1, provided

$$\left(\frac{\varrho_M}{\varrho_w}\right)\frac{\mathcal{H}_w}{\mathcal{H}_o} \ll 1 \ .$$

However, since our wiggler can only be mounted in a straight section (where η = 2 m) the above ratio is always >1. From the point of view of synchrotron radiation the effect may be undesirable but is always very small around ϱ_w = 2.78 m, where the machine will mostly be used for this application. From the point of view of two-beam operation (to be discussed in the following), the enlargement of the emittance together with the lower β_z value at the crossing point in principle allowsa higher luminosity to be obtained (expecially towards the low energy side of the operating range) in two of the four experimental regions.

The unperturbed machine parameters to be put into formulas (67) through (70) are listed in Table II, for operating point 3.2, 5.2.

TABLE II

β^*(m)	10.7
β_2^*(m)	0.778
σ_{p_o}	$3.910^{-4} E_{GeV}$
$\mathcal{H}_o$(m)	0.304
η(m)	2.05
ϱ_M(m)	5
l_M(m)	31.42
l_w(m)	1.603

It may also be useful to recall that

$$\sigma_{x\beta_o} = \sigma_{p_o}\left(\frac{2}{1+k^2}\,\mathcal{H}_o\beta_x\right)^{1/2} ,$$

$$\sigma_{x_o} = \sigma_{p_o}\left(\eta^2 + \frac{2}{1+k^2}\mathcal{H}_o\beta_x\right)^{1/2} , \qquad (71)$$

$$\sigma_{z_o} = k\,\sigma_x\beta_o\left(\frac{\beta_z}{\beta_x}\right)^{1/2} \quad \text{or} \quad \frac{\varepsilon_{z_o}}{\varepsilon_{x\beta_o}} = k^2 ,$$

where k is a coupling coefficient that becomes 1 in full coupling. The minimum value of k^2 is not easily determined but is estimated to be now in the range of 1-5 x 10^{-2}, and is expected to become somewhat larger when the wiggler is turned on.

In the most unfavourable case, k = 1 (full coupling), the unperturbed emittaces are (Table III).

TABLE III

Q_x, Q_2	3.1, 3.1	3.2, 5.2
ε_{x_o} (m x rad)	$1.33 \times 10^{-7} E^2$ (GeV)	$1.06 \times 10^{-7} E^2$ (GeV)
ε_{z_o} (m x rad)	$5.9 \times 10^{-8} E^2$ (GeV)	$4.6 \times 10^{-8} E^2$ (GeV)

Emittances at the usual operating point (3.1, 3.1) have been added for comparison.

II.5. - Colliding beams operation.

It has been shown in sec. II.4 that wigglers modify the beam emittance. In particular, in our case, the large increase in beam emittance for small values of ϱ_w affords the possibility of increasing the storage ring luminosity at low energy.

In order however to be able to operate the ring in the colliding beam mode, two conditions have to be met:

a) the wiggler must be matched into the structure;
b) the phase shift between two adjacent crossing regions must be the same for all crossings and must be equal to $n\pi + \delta$, with $\delta \ll 1$.

Condition a) means, as shown earlier, that the ring has to be operated at $Q_z = 5.2$. Condition b) requires the ring to be operated with one bunch per beam and with at least two wigglers, symmetrically placed with respect to the X-ing regions (due to the θ^* introduced by each wiggler). The effects of two wigglers on the machine parameters are shown in Fig. 13b. The luminosity obtainable at operating point "3.2, 5.2" with one bunch per beam and without wigglers is shown in Fig. 14, curve A. It has been assumed that the maximum current that can be stored in a single bunch is 33 mA, and we believe that this is a somewhat conservative assumption. Curve A is compared to the luminosity obtainable at "3.05, 3.05" with three bunches per beam, assuming that, with the new RF, 100 mA can be stored in three bunches (curve B).

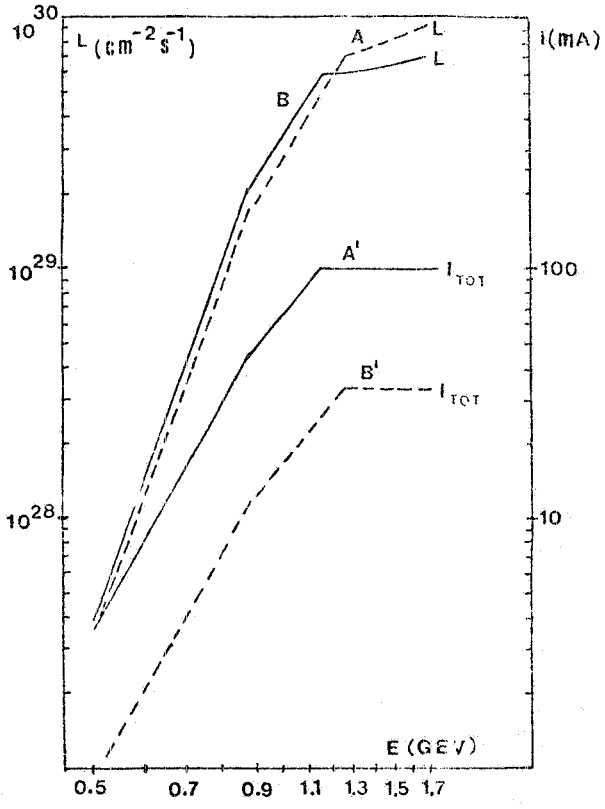

A, A': 1 Bunch/beam; Q_x=3.2, Q_z=5.2
B, B': 3 Bunches/beam; $Q_x \cong 3.1$, $Q_z \cong 3.1$.

FIG. 14

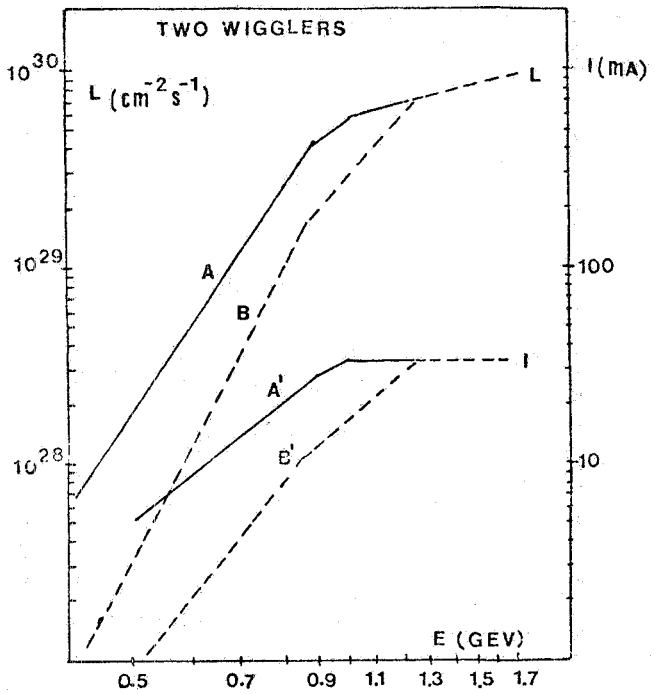

for $E > 884$ MeV $\quad \xi_{MAX} = 0.056$

$E < 884$ MeV $\quad \xi_{MAX} = 0.056 \left(\frac{E}{884}\right)^{1.5}$

$I_{lim} = 33.3$ mA

A, A': wigglers on; B, B': wigglers off.

FIG. 15

Since luminosity is proportional to

$$\frac{b}{\beta_z} \qquad b = \text{number of bunches}$$

and b/β_z is approximately the same for the two operating points, the two curves are almost superimposed at low energies. The lower value of β_z for the $Q_z = 5.2$ case allows a higher charge density to be obtained so that at high energy, where the current limit sets in, the one-bunch luminosity is slightly higher.

The maximum storable currents for the two cases are also plotted in Fig. 14 (curves A', B'). Fig. 15 shows how luminosity could be increased over that indicated by curve A of Fig. 14, if two wiggler magnets were installed. It is assumed that the wigglers can be run at full field (18 KG) from 0.54 GeV up. Above 1.25 GeV the wigglers may be turned off if one is limited, as indicated in the figure, by the storable current.

We believe this calculation to be conservative from at least two points of view:

- It is likely that more that 30 mA can be reliably stored in a single bunch.
- The $E^{1.5}$ experimental dependence of ξ on energy[8] below ~ 0.9 GeV is likely to be related to the machine damping time.

Since the wigglers cause the damping time to decrease by about a factor of four at ~ 500 MeV, it is not unlikely that luminosity at that energy could increase by another factor of ~ 2 over that estimate. As far as bunch lengthening is concerned, we have calculated what the source length would be, due to anomalous lengthening, with the new 50 MHz RF and with the current versus energy law given in Fig. 15 (Curve A'). The results of the calculation is shown in Fig. 16.

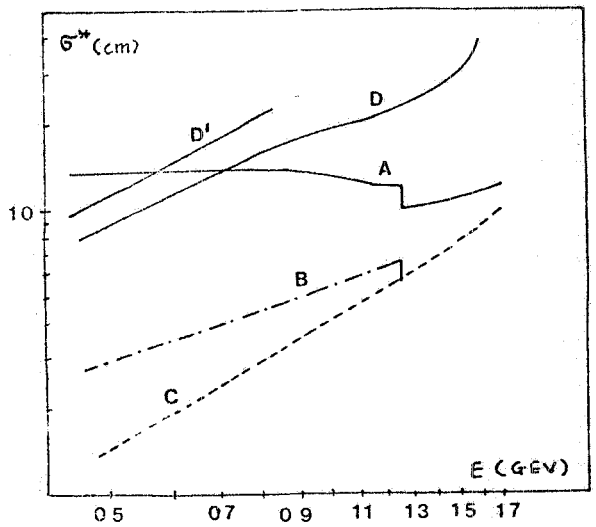

Curve A V_{RF} = 250 KV, h = 18

Curve B σ^*_{RAD} (2 wigglers)

Curve C σ^*_{RAD} (wiggler off)

Curve D V_{RF} = 140 KV, h = 3

Curve D' V_{RF} = 60 KV, h = 3 .

FIG. 16

In Fig. 16, curves B and C show the natural source length with and without wigglers. Curves D and D' are shown for reference, and give the present source length at 140 KV and 60 KV respectively.

For the sake of completeness it should be added that operation at point "3.2, 5.2" will require the installation of two new pairs of beam separator electrodes in two pairs of quadrupoles near an interaction region, since the present electrode arrangement is not adequate on the new operating point. It is possible to install the new electrodes so that the beam separation is maximum in the interaction region and becomes about one half of the maximum at the wiggler locations.

The aperture (at the wiggler) required for separating the beams at injection is thus less than that required under normal operating conditions (3.1, 3.1 ; wigglers off) for a given separation.

The vertical beam dimension at the edge of the wiggler straight section is, in the worst case (1.25 GeV, wigglers at full field, full coupling) :

$$\sigma_z = 0.6 \text{ mm} .$$

The available vertical aperture without separation, allowing for a $\pm$ 5 mm closed orbit (very conservative), is therefore $\sim 35\,\sigma_z$, which is slightly better than that available under normal operating conditions.

ACKNOWLEDGEMENTS. -

B. Dulach has designed the mechanics of magnet and coils. A. Hofmann (CERN) and M. Ricci (CNEN) have been of great assistance in running field mapping programs.

Useful discussions with H. Winick (SLAC) and with all members of the Adone group are gratefully acknowledged.

REFERENCES. -

(1) - A. Hofmann, R. Little, J. M. Peterson, K. W. Robinson, G. A. Voss and H. Winick, Proc. VIth Intern. Conf. on High Energy Accelerators, Cambridge (1967).
(2) - E. M. Rowe, private communication.
(3) - W. W. Ash et al., Description and performance of MEA, the magnetic detector at Adone, Frascati report LNF-77/18 (1977).
(4) - PULS, Programma per l'utilizzazione della luce di sincrotrone, LNF-PULS publication (1976).
(5) - M. Bassetti, Variable curvature function storage rings. Dimensions and damping control, T-66 INT. MEMO (1974), unpublished; J. M. Peterson, J. R. Rees and H. Wiedermann, Control of beam size and polarization time in PEP, Report PEP-125/SPEAR-186 (1975).
(6) - A. Hutton, Control of the low energy characteristics of the LSR electron ring using wiggler magnets, Part. Acc. 7, 3 (1976).
(7) - M. Sands, The physics of electron storage rings. An introduction, Report SLAC-121 (1970).
(8) - F. Amman, M. Bassetti, A. Cattoni, V. Chimenti, D. Fabiani, M. Matera, C. Pellegrini, M. Placidi, M. Preger, A. Renieri, S. Tazzari, F. Tazzioli and G. Vignola, Proc. VIIIth Intern. Conf. on High Energy Accelerators, CERN (1971).
(9) - H. Winick, Proc. Course on Synchrotron Radiation Reserach, International College on Applied Physics, Alghero (1976), vol. I, pag. 1.

APPENDIX I

From matrix (32) it can be deduced that

$$\beta^{*2} = \beta^2 - 2nl\beta\,\mathrm{cotgn}\,\theta - (nl)^2 ,$$

and therefore limit

$$\beta^{*2}_{as} = \lim_{\theta \to 0} \left[\beta^2 - 2nl\beta\,\mathrm{cotgn}\,\theta - (nl)^2\right] \tag{A1}$$

has to be found, subject to condition

$$l = l_1 + l_2 ,$$

and with $\beta(k)$, $\theta(k)$ defined by the matrix (see (35))

$$\begin{vmatrix} \cos\theta & \beta\sin\theta \\ -\dfrac{\sin\theta}{\beta} & \cos\theta \end{vmatrix} = \begin{vmatrix} 1 - 2(kl - k^2 l_1 l_2) & 2\left[(l_1 + l_2) - k(l_1 l + l_1 l_2 + k^2 l_1^2 l_2\right] \\ -2k(1 - kl_2) & 1 - 2(kl - k^2 l_1 l_2) \end{vmatrix} \tag{A2}$$

Let us expand $k(\theta)$ as follows

$$k \simeq p\theta^2(1 + q\theta^2) , \tag{A3}$$

From equality

$$\cos\theta = 1 - 2(kl - k^2 l_1 l_2)$$

one can deduce, by equating the coefficients of equal powers of θ,

$$p = \frac{1}{4l} \quad , \qquad q = \frac{l_1 l_2 - l_1^2 - l_2^2}{12l^2} \tag{A4}$$

On the other hand, from (A2) it follows that

$$\beta^2 = \frac{(l_1 + l_2) - k(l_1 l + l_1 l_2) + k^2 l_1^2 l_2}{k(1 - kl_2)}$$

and, by a series expansion in powers of k,

$$\beta^2 = \frac{l_1 + l_2}{k}\left[1 - k\left(\frac{l_1 l + l_1 l_2}{l} - l_2\right) + k^2\left(\frac{l_1^2 l_2}{l} + l_2^2 - \frac{(l_1 l + l_1 l_2)}{l} l_2 + \cdots\right)\right] \tag{A5}$$

Last, by substituting (A3) into (A5) one obtains

$$\beta^2 = \frac{4l^2}{\theta^2}\left[1 + \frac{\theta^2}{6l^2}(2l_2^2 - 2l_1 l_2 - l_1^2) + \cdots\right]$$

and obviously

$$\beta = \frac{2l}{\theta}\left[1 + \frac{\theta^2}{12l^2}(2l_2^2 - 2l_1l_2 - l_1^2) + \cdots\right] \tag{A6}$$

Since

$$\operatorname{cotg} n\theta \simeq \frac{1}{n\theta}\left(1 - \frac{n^2}{3}\theta^2\right) \tag{A7}$$

one eventually obtains, by substitution of (A6) and (A7) into (A1)

$$\beta_{as}^{*2} = \frac{(n^2 - 1)l^2}{3} + l_2^2 \ . \tag{A8}$$

APPENDIX II

The additional β-function, $\beta_w - \beta_o$, that propagates around the machine (when there is a mismatch) with a periodicity that is no longer that of the unperturbed machine, can be found as follows.

Define an initial matrix, associated with function β as follows:

$$A(0) = \begin{vmatrix} \gamma & \alpha \\ \alpha & \beta \end{vmatrix} \tag{A9}$$

If T(s) is the transport matrix from the starting point to point s, it can be easily shown that

$$A(s) = (T_{(s)}^{-1})^T A(0)\, T_{(s)}^{-1} \tag{A10}$$

Since at the symmetry point (e.g. the point opposite to the wiggler) α is always zero, one can write

$$\begin{vmatrix} 1/\beta_w & 0 \\ 0 & \beta_w \end{vmatrix} = \begin{vmatrix} 1/\beta_o & 0 \\ 0 & \beta_o \end{vmatrix} + \begin{vmatrix} \left(\frac{1}{\beta_w} - \frac{1}{\beta_o}\right) & 0 \\ 0 & (\beta_w - \beta_o) \end{vmatrix} \tag{A11}$$

so that, for the extra propagating function $(\beta_w - \beta_o)$ one may write

$$\begin{vmatrix} \Delta\gamma(s) & \Delta\alpha(s) \\ \Delta\alpha(s) & \Delta\beta(s) \end{vmatrix} = \begin{vmatrix} a_{22} & -a_{21} \\ -a_{12} & a_{11} \end{vmatrix} \begin{vmatrix} \left(\frac{1}{\beta_w} - \frac{1}{\beta_o}\right) & 0 \\ 0 & (\beta_w - \beta_o) \end{vmatrix} \begin{vmatrix} a_{22} & -a_{12} \\ -a_{21} & a_{11} \end{vmatrix} \tag{A12}$$

and, taking into account element $\Delta\beta(s)$ only, one obtains

$$\Delta\beta(s) = (\beta_w - \beta_o)\left[a_{11}^2 - \frac{a_{12}^2}{\beta_w \beta_o}\right] \tag{A13}$$

In (A13) it has to be remembered that elements a_{11} and a_{12} are relative to trajectory interval $0 \rightarrow s$, and are not those of the one-turn matrix relative to point s. As well known the transport matrix from 0 to s can be written, under the assumption that 0 is a symmetry point:

$$T(s) = \begin{vmatrix} \sqrt{\frac{\beta(s)}{\beta_o}} \cos\mu(s) & \sqrt{\beta_o \beta(s)} \sin\mu(s) \\ -\frac{\sin\mu(s) + \alpha(s)\cos\mu(s)}{\sqrt{\beta_o \beta(s)}} & \sqrt{\frac{\beta_o}{\beta(s)}} \left[\cos\mu(s) - \alpha(s) \sin\mu(s)\right] \end{vmatrix} \tag{A14}$$

so that (A12) becomes

$$\Delta\beta(s) = \frac{\beta(s)}{\beta_o} (\beta_w - \beta_o) \left[1 - \sin^2\mu(s) \left(1 + \frac{\beta_o}{\beta_w}\right)\right] . \tag{A15}$$

From (A15) it follows that, for $\sin^2\mu(s) = 1$, $\Delta\beta(s)$ changes sign with respect to the starting value, and is given by

$$\Delta\beta(\sin^2\mu = 1) = -\frac{\beta(s)}{\beta_w} (\beta_w - \beta_o) .$$

In conclusion one may write :

$$\frac{\beta(s)}{\beta_w} (\beta_o - \beta_w) < \Delta\beta(s) < (\beta_w - \beta_o) \frac{\beta(s)}{\beta_o} \qquad \text{if} \quad \beta_w > \beta_o$$

or

$$\frac{\beta(s)}{\beta_o} (\beta_w - \beta_o) < \Delta\beta(s) < (\beta_o - \beta_w) \frac{\beta(s)}{\beta_w} \qquad \text{if} \quad \beta_w < \beta_o \quad . \tag{A16}$$